BIOCHEMISTRY
including biophysical chemistry & molecular biology
Article

Biochemistry **2011,** *50,* 1607–1617 1607
DOI: 10.1021/bi1013744

A Kinetic Aggregation Assay Allowing Selective and Sensitive Amyloid-β Quantification in Cells and Tissues[†]

Deguo Du,[§] Amber N. Murray,[§] Ehud Cohen,[‡] Hyun-Eui Kim,[‡] Ryan Simkovsky,[§] Andrew Dillin,[‡] and Jeffery W. Kelly*[,§]

[‡]*Howard Hughes Medical Institute, Molecular and Cell Biology Laboratory, The Salk Institute for Biological Studies, 10010 North Torrey Pines Road, La Jolla, California 92037, United States, and* [§]*Departments of Chemistry and Molecular and Experimental Medicine and The Skaggs Institute for Chemical Biology, The Scripps Research Institute, 10550 North Torrey Pines Road, La Jolla, California 92037, United States*

Received August 25, 2010; Revised Manuscript Received December 28, 2010

ABSTRACT: The process of amyloid-β (Aβ) fibril formation is genetically and pathologically linked to Alzheimer's disease (AD). Thus, a selective and sensitive method for quantifying Aβ fibrils in complex biological samples allows a variety of hypotheses to be tested. Herein, we report the basis for a quantitative in vitro kinetic aggregation assay that detects seeding-competent Aβ aggregates in mammalian cell culture media, in *Caenorhabditis elegans* lysate, and in mouse brain homogenate. Sonicated, proteinase K-treated Aβ fibril-containing tissue homogenates or cell culture media were added to an initially monomeric Aβ_{1-40} reporter peptide to seed an in vitro nucleated aggregation reaction. The reduction in the half-time (t_{50}) of the amyloid growth phase is proportional to the quantity of seeding-competent Aβ aggregates present in the biological sample. An ion-exchange resin amyloid isolation strategy from complex biological samples is demonstrated as an alternative for improving the sensitivity and linearity of the kinetic aggregation assay.

In Alzheimer's disease (AD),[1] the most common human neurodegenerative disorder, enzyme-mediated endoproteolysis of the amyloid precursor protein (APP) in the secretory and endocytic pathways produces a family of closely related peptides collectively termed the amyloid-β peptide (Aβ). Compelling genetic and pathological evidence indicates that AD is mechanistically linked to the production and aggregation of Aβ, particularly Aβ_{1-42} (*1*−*3*). Another major risk factor for the development of AD is aging (*4*−*6*).

No drugs that alter disease progression are approved for AD. When such treatments become available, it is likely that their efficiency will be critically dependent upon early diagnosis, as substantial neuronal cell loss and brain volume decreases occur during the intermediate stages of AD. Intracellular tau tangles are also observed in AD (*7*, *8*), suggesting there may be a more general loss of proteostasis (*5*, *6*, *9*−*13*). At present, routine methods for specifically detecting Aβ aggregates and tau deposits before autopsy are not available, and while some progress is being made in the detection of extracellular Aβ (*14*−*17*), these compounds usually bind to amyloid fibrils composed of several different proteins, making a definitive diagnosis more challenging (*18*). Thus, a highly sensitive and selective methodology for the quantitative detection of Aβ aggregates in cells, animal models, and living patient tissue and biological fluids would be welcomed.

Aβ amyloidogenesis appears to proceed by a nucleated polymerization mechanism in vitro (*19*−*23*). The rate-limiting step of this process is the formation of an oligomeric nucleus, the highest-energy species on the amyloidogenesis pathway, formation of which is required before fibril formation becomes thermodynamically favorable (Figure 1a). Once a nucleus is formed, additional monomeric Aβ peptides or oligomers can be added to the fibril in a step that is thermodynamically favorable, leading to a fast growth phase (Figure 1a, inset) (*21*). Once the monomer concentration is depleted below the critical concentration, the amyloidogenesis reaction enters a stationary phase (Figure 1a, inset). The duration of the lag phase associated with nucleation is reduced in proportion to the quantity of preformed amyloid fibrils, or seeds, added to an in vitro aggregation reaction mixture (Figure 1a, inset) (*23*), and this is the basis of our kinetic aggregation assay.

We have previously used the half-time (t_{50}) of the growth phase of the in vitro Aβ amyloidogenesis reaction to semiquantitatively detect the seeding-competent Aβ aggregates, including amyloid in tissue homogenates from *Caenorhabditis elegans* and murine AD models (*5*, *6*). Herein, we report a substantially optimized kinetic aggregation assay that features new procedures that make the assay more reliable and importantly allows for the quantification of the seeding-competent Aβ aggregate load in tissues and in cells. The kinetic aggregation assay is at least 3 orders of magnitude more sensitive than a Western blot without antigen retrieval in quantifying the Aβ aggregate load in mouse and worm tissue. Unlike the small molecules that semiquantify the amyloid load via PET imaging (*14*), the kinetic aggregation assay does not sensitively detect amyloid composed of other proteins.

EXPERIMENTAL PROCEDURES

Preparation of Seed-Free Aβ Peptide. Aβ_{1-40} was synthesized using standard Fmoc chemistry for solid phase peptide synthesis (*24*). The resulting peptide was purified by reversed phase C18 high-performance liquid chromatography (RP-HPLC) and

[†]This research was supported by National Institutes of Health Grant AG031097, The Skaggs Institute for Chemical Biology, and the Lita Annenberg Hazen Foundation.

*To whom correspondence should be addressed. Phone: (858) 784-9601. Fax: (858) 784-9610. E-mail: jkelly@scripps.edu.

[1]Abbreviations: Aβ, amyloid-β peptide; AD, Alzheimer's disease; AFM, atomic force microscopy; APP, amyloid precursor protein; CSF, cerebrospinal fluid; EV, empty vector; PBS, phosphate-buffered saline; PDS, post-debris supernatant; PK, proteinase K; PI, complete protease inhibitor cocktail; RP-HPLC, reversed phase high-performance liquid chromatography; RT, room temperature; SD, standard deviation; ThT, thioflavin T; WT, wild type.

Published on Web 01/26/2011

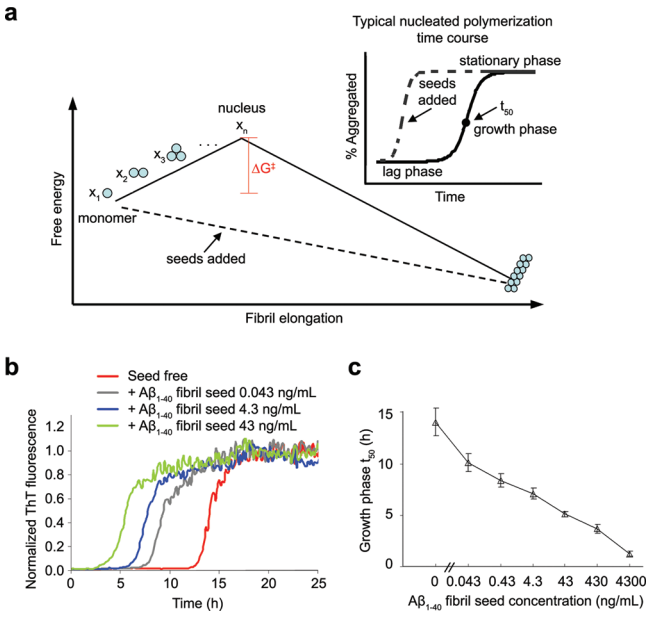

FIGURE 1: Effect of addition of preformed $A\beta_{1-40}$ or $A\beta_{1-42}$ fibrils on an $A\beta_{1-40}$ amyloidogenesis reaction (basis for the $A\beta_{1-40}$ kinetic aggregation assay). (a) Free energy amyloidogenesis reaction coordinate diagram for the nucleation-dependent aggregation of $A\beta_{1-40}$ (—). Addition of a sufficient quantity of preformed $A\beta_{1-40}$ fibrils or seeds (---) eliminates the requirement for nucleation, which is the rate-limiting step for $A\beta_{1-40}$ amyloidogenesis. The inset shows a typical nucleated polymerization time course. The addition of amyloid fibril seeds reduces the t_{50} in proportion to the quantity of seed termini added. (b) $A\beta_{1-40}$ (10 μM) aggregation kinetics (pH 7.4, 37 °C) with agitation (shaking for 5 s every 10 min) in the absence or presence of the indicated amount of preformed $A\beta_{1-40}$ fibril seeds (sonicated for 40 min before addition). The amyloidogenesis reaction is followed by the binding of ThT to the fibril, which dramatically increases its fluorescence quantum yield. Fluorescence is normalized to the value of the plateau phase in a given reaction. (c) Observed amyloidogenesis t_{50} as a function of the amount of $A\beta_{1-40}$ fibril seed added. Data are reported as means ± SD of triplicate results.

characterized by matrix-assisted laser desorption ionization mass spectrometry. The $A\beta_{1-40}$ peptide utilized in the kinetic aggregation assay was monomerized as described previously (*25*). Briefly, lyophilized Aβ powder was dissolved in aqueous NaOH (2 mM), and the pH was adjusted to 10.5 with aqueous NaOH (100 mM). The solution was sonicated (20 min, 25 °C) and then filtered sequentially through 0.2 μm and 10 kDa cutoff filters. The concentration of protein was determined by UV absorbance at 280 nm (ε = 1280 M^{-1} cm^{-1}). The final peptide solution was seed-free as determined by atomic force microscopy (AFM) and dynamic light scattering analysis.

Strains of Mice and Preparation of Brain Homogenate. An AD mouse model expressing both a mutant chimeric mouse/human APP_{swe} and a mutant human presenilin 1 (ΔE9), both driven by the prion protein promoter, was purchased from Jackson Laboratory [strain B6C3-Tg (APP_{swe} PSEN1dE9) 85Dbo/J, stock number 004462]. Long-lived male mice harboring only one *Igf1r* copy (*26*) were obtained from J. Friedman (The Scripps Research Institute, La Jolla, CA). Details of crosses and genotyping are provided as Supporting Information. Mouse brain was homogenized in cold PBS using a glass tissue grinder (885482, Kontes, Vineland, NJ) to a final concentration of 10% (w/v) and then centrifuged at 1000g for 3 min. The total protein concentration in mouse brain homogenate was measured with a BCA kit (Pierce, Rockford, IL).

Worm Growth and Preparation of PDS. Wild-type (N_2) and CL2006 Aβ worm strains were obtained from the *Caenorhabditis* Genetics Center (Minneapolis, MN). Worms were grown on bacterial strains at 20 °C. At day 1 of adulthood, the worms were washed twice with M9 medium and once more with phosphate-buffered saline (PBS) (room temperature), resuspended in 300 μL of ice-cold PBS, transferred to a 2 mL tissue grinder (885482, Kontes), and homogenized. Crude homogenates were spun in a desktop microfuge (3000 rpm, 3 min), and the resulting supernatant, the post-debris supernatant (PDS), was transferred to new tubes and the total protein concentration measured with a BCA kit (Pierce).

APP-Overexpressing Cell Lines. Genes encoding human wild-type APP (APP_{wt}) and APP carrying the Swedish mutations (APP_{swe}) were cloned into the tetracycline-inducible mammalian expression vector pcDNA4/TO (Invitrogen). T-REx-293 cells (Invitrogen) were stably transfected with empty pcDNA4/TO (EV), pcDNA4/TO/APP_{wt}, or pcDNA4/TO/APP_{swe} vector. Following transfection, clones were selected and subcloned to ensure genetic homogeneity. For expression, 3×10^6 cells adhered to 10 cm plates overnight, after which 100 ng/mL tetracycline (Sigma-Aldrich) was added to the culture medium to induce overexpression. Conditioned culture media were aspirated from individual culture plates over the course of 4 days following tetracycline induction and stored at −20 °C. The total protein concentration in cell culture media was measured with a BCA kit (Pierce). See the Supporting Information for details of the cloning and cell culture.

Preparation of $A\beta_{1-40}$ Seeds. $A\beta_{1-40}$ fibrillar seeds were prepared by incubation of a monomerized $A\beta_{1-40}$ peptide solution (50 μM) in phosphate buffer [50 mM sodium phosphate and 150 mM NaCl (pH 7.4)] at 37 °C in a 1.5 mL reaction tube on a rotating shaker (20 rpm) for 5−6 days. Fibril morphology was confirmed by AFM analysis (see the Supporting Information for details of AFM).

In Vitro $A\beta_{1-40}$ Kinetic Aggregation Assay with Added Preformed $A\beta_{1-40}$ Seeds. The preformed $A\beta_{1-40}$ fibrils were sonicated for 40 min in a water bath sonicator (FS60, Fisher Scientific, Pittsburgh, PA). A known quantity of these seeds was added to a monomerized $A\beta_{1-40}$ peptide solution diluted to a final concentration of 10 μM in phosphate buffer [50 mM sodium phosphate and 150 mM NaCl (pH 7.4)] containing ThT (20 μM). Three aliquots (100 μL) were transferred into wells of a 96-well microplate (Costar #3631, black, clear bottom), and the plate was sealed with a microplate cover and loaded into a Gemini SpectraMax EM fluorescence plate reader (Molecular Devices, Sunnyvale, CA), where it was incubated at 37 °C. The fluorescence (excitation at 440 nm, emission at 485 nm) was measured from the bottom of the plate at 10 min intervals, with agitation for 5 s before each reading. The half-maximal fluorescence time point (t_{50}) was defined as the time point at which ThT fluorescence reached the midpoint between pre- and postaggregation baselines. t_{50} values represent means of triplicate results.

In Vitro $A\beta_{1-40}$ Kinetic Aggregation Assay with Added Aβ Fibril-Doped Biological Samples. Preformed $A\beta_{1-40}$ fibrils were added to mouse brain homogenates or worm PDS in known amounts, and the mixture was sonicated for 40 min in an ice/water bath before being added to an $A\beta_{1-40}$ monomer solution (10 μM) for the kinetic aggregation assay. For the treatment with proteinase K (PK), samples spiked with known amounts of preformed $A\beta_{1-40}$ amyloid were sonicated for 40 min in an ice/water bath and then incubated with PK (w/w ratio of

PK to total protein in the sample of 1:500) for 2 h at 25 °C. The solution was then supplemented with Roche complete protease inhibitor cocktail (PI) (catalog no. 1836170) at a concentration 4 times the recommended concentration to inhibit PK activity. The mixed solution was then sonicated for 20 min and added to the kinetic aggregation assay. The concentration of total protein from the mouse brain homogenate or worm PDS in the kinetic aggregation assay was 10 μg/mL.

In Vitro Aβ_{1-40} Kinetic Aggregation Assay with Other Biological Samples. For assays with PK treatment, samples were sonicated for 20 min (N_2 and Aβ worm PDS, and cell culture media) or 40 min (WT and AD mouse brain homogenates) in an ice/water bath and treated for 2 h with PK at 25 °C (w/w ratio of PK to total protein in the sample of 1:500), and then PI was added at a concentration 4 times the recommended concentration to inhibit PK activity. The mixed solution was sonicated for an additional 20 min and then added to the kinetic aggregation assay. The concentration of total protein in the final kinetic aggregation assay was 10 μg/mL (mouse brain homogenate and worm PDS) and 25 μg/mL (cell culture media). For the assays without PK and PI treatment, samples were sonicated for 20 min (worm PDS and cell culture media) or 40 min (mouse brain homogenate) before being added to the kinetic aggregation assay.

Aβ amyloid Ion-Exchange Isolation. Preformed Aβ_{1-40} amyloid (13 ng) was suspended in 200 μL of H_2O, sonicated for 40 min in an ice/water bath, and then incubated with 8 μL of weak cation CM beads (CM Sepharose fast flow, GE) in a 0.6 mL microcentrifuge tube on a rotating shaker (10 rpm) overnight at 4 °C. The CM beads were washed three times with H_2O and then added to the kinetic aggregation assay. To isolate the Aβ_{1-40} amyloid doped into mouse brain homogenate, preformed Aβ_{1-40} fibrils were added to WT mouse brain homogenate samples in known amounts (total protein concentration from mouse brain homogenate of 15 μg/mL). The mixture was sonicated for 40 min in an ice/water bath and then incubated with 8 μL of CM beads in 200 μL of H_2O in a 0.6 mL microcentrifuge tube on a rotating shaker (10 rpm) overnight at 4 °C. The CM beads were washed three times with H_2O and then added to the kinetic aggregation assay. To isolate endogenous Aβ_{1-40} amyloid in WT and AD mouse brain homogenates, homogenates prepared as described above (total protein concentration from mouse brain homogenate of 50 μg/mL) were sonicated for 40 min in an ice/water bath and then incubated with 8 μL of CM beads in 200 μL of H_2O in a 0.6 mL microcentrifuge tube on a rotating shaker (10 rpm) overnight at 4 °C. The beads were washed three times with H_2O and added to the kinetic aggregation assay.

Western Blot. Worm PDS or mouse brain homogenate samples spiked with added Aβ_{1-40} fibril seed were boiled with sodium dodecyl sulfate loading buffer for 10 min and then were loaded onto sodium dodecyl sulfate−polyacrylamide gel electrophoresis (SDS−PAGE) gels and blotted onto nitrocellulose paper. The blots were incubated with primary antibody 6E10 (Covance, San Diego, CA) at a 1:10000 dilution overnight and then incubated with secondary goat anti-mouse HRP-conjugated antibody (Pierce) at a 1:10000 dilution. Blots were visualized by enhanced chemiluminescence using SuperSignal West Pico Substrate (Pierce).

RESULTS

Sonicated Aβ_{1-40} Amyloid Fibrils Dose-Dependently Accelerate Aβ_{1-40} Amyloidogenesis in Vitro. To evaluate the influence of known quantities of sonicated Aβ_{1-40} amyloid fibrils or seeds on the in vitro amyloidogenesis kinetics of an initially monomeric Aβ_{1-40} peptide (10 μM), we compared the Aβ_{1-40} lag phase duration as a function of the amount of added Aβ_{1-40} fibrillar seeds (prepared as described in Experimental Procedures) in phosphate buffer [50 mM sodium phosphate and 150 mM NaCl (pH 7.4)] containing thioflavin (ThT, 20 μM). These experiments were conducted in a 96-well microtiter plate (Costar catalog no. 3631, black, clear bottom) housed in a fluorescent plate reader over the time course of the experiment (37 °C). The fluorescence at 485 nm was measured from the bottom of the plate at 10 min intervals, with agitation for 5 s before each reading. The Aβ_{1-40} fibrils (Figure S1a of the Supporting Information) were sonicated in a water bath sonicator for 40 min to generate a more uniform (70−150 nm) length distribution (Figure S1b of the Supporting Information), based on AFM imaging. Because seeding has been shown to be mediated by the fibril ends (*27*, *28*), sonication to afford a uniform length distribution is critical for the ability to quantify the amount of fibrils of different lengths in tissues or cells. The time course of Aβ_{1-40} fibril formation in vitro was monitored using ThT fluorescence. ThT is an environmentally sensitive fluorophore, whose selective binding to amyloid fibrils dramatically increases its fluorescence quantum yield (*29*).

Addition of sonicated Aβ fibrils or nuclei shortens the lag phase of Aβ amyloidogenesis (Figure 1b). This is most conveniently measured as the half-time (t_{50}) of the growth phase, which is defined as the time at which the fluorescence intensity reaches the midpoint between the pre- and postaggregation baselines (Figure 1a, inset). We sonicated Aβ_{1-40} amyloid for 40 min to prepare seeds, as longer sonication does not further reduce the t_{50} appreciably. The kinetic aggregation assay is based on the hypothesis that the aggregation half-time of the growth phase is proportional to the amount of sonicated Aβ fibrils added (Figure 1b). As shown in Figure 1c, the growth phase t_{50} quantitatively correlates with the quantity of sonicated Aβ_{1-40} fibril seeds added to the in vitro kinetic aggregation assay, confirming the predicted quantitative effect of seeding on the lag phase of Aβ_{1-40} fibrillization in vitro (*19*−*23*). This quantitative relationship is the first innovation we report, which makes this assay more valuable, as previously it was employed to simply demonstrate that there were aggregates present in the sonicated tissue.

A quantitative kinetic aggregation assay should be highly selective; i.e., Aβ amyloidogenesis should not be seeded by amyloids of distinct sequence (*30*, *31*). Sonicated α-synuclein fibrils (14.5 μg/mL final concentration) formed from the α-synuclein monomer (50 μM) have less seeding capacity than 4.3 ng/mL Aβ_{1-40} fibrils, making them $<1/1000$ as seeding-competent as Aβ fibrils (Figure S2a of the Supporting Information). Sonicated 8 kDa gelsolin fibrils (7.9 μg/mL final concentration) formed from the 8 kDa gelsolin monomer (50 μM) have a seeding capacity equivalent to that of 43 ng/mL Aβ_{1-40} fibrils, making them 1/100 as seeding-competent as Aβ fibrils (Figure S2b of the Supporting Information). Therefore, the Aβ_{1-40} kinetic aggregation assay exhibits the selectivity expected of an assay that will be used to quantify Aβ fibril load in tissues that could possibly have other amyloids present. In contrast to α-synuclein and 8 kDa gelsolin, the sequence of the islet amyloid polypeptide (IAPP) exhibits substantial homology with Aβ_{1-40}. However, it is established that IAPP fibrils exhibit weight-normalized efficiencies of only 1−2% relative to Aβ_{1-40} seeding

of $A\beta_{1-40}$ amyloidogenesis (*30*). Moreover, IAPP is not expressed in the brain of mice. For these reasons, it is very unlikely that cross seeding of $A\beta_{1-40}$ amyloidogenesis by IAPP fibrils would be problematic in the work presented here.

To confirm that ThT fluorescence accurately reflects the amount of aggregates formed and to verify that there are no nonfluorescent or weakly fluorescent aggregates present, we chose to quantify the amount of Aβ aggregates formed following seeding by RP HPLC. A 150000*g* ultracentrifugation for 1 h successfully separates soluble Aβ monomers from pelleted Aβ fibrils and aggregates (Figure S2c of the Supporting Information). When the kinetic aggregation assay reached the stationary phase, samples were spun at 150000*g*, and the total amount of $A\beta_{1-40}$ present in pellets was quantified by RP HPLC. Seeding with 14.5 μg/mL α-synuclein fibrils yields the same amount of pelletable $A\beta_{1-40}$ as seeding with 4.3 ng/mL $A\beta_{1-40}$ fibrils (Figure S2d of the Supporting Information). Likewise, seeding with 7.9 μg/mL 8 kDa gelsolin fibrils yields the same amount of pelletable $A\beta_{1-40}$ as seeding with 43 ng/mL $A\beta_{1-40}$ fibrils (Figure S2e of the Supporting Information). These data support the hypothesis that nonhomologous seeds are not facilitating the formation of nonfibrillar Aβ aggregates.

While the $A\beta_{1-40}$ and $A\beta_{1-42}$ amyloid structures are subtly different (*32*−*34*), it is well-established that $A\beta_{1-40}$ takes on the structure of the $A\beta_{1-42}$ fibril when seeded with sonicated $A\beta_{1-42}$ fibrils (*35*, *36*). Because the aggregation of $A\beta_{1-42}$ from a monomeric solution is dramatically faster than that of $A\beta_{1-40}$, without an obvious lag phase (*35*), we utilized the $A\beta_{1-40}$ peptide as the readout peptide in the kinetic aggregation assay to detect aggregates of $A\beta_{1-40}$ and/or $A\beta_{1-42}$ that are competent for seeding $A\beta_{1-40}$ fibrillization. In principle, shorter Aβ peptides could also be used as the readout peptide in the kinetic aggregation assay, although this was not explored. To minimize the influence of the other components in cell or tissue homogenates on the observed t_{50} in the $A\beta_{1-40}$ kinetic aggregation assay, two methods were employed: proteinase K treatment to degrade the soluble proteome and ion-exchange capture of amyloid to beads so that the soluble proteome, membrane components, and other components can be washed away.

Proteinase K Treatment of Tissue Homogenates Improves Quantitative Linearity. To assess whether the $A\beta_{1-40}$ kinetic aggregation assay can be used to quantify the amount of Aβ fibrils in a given tissue or cell, we first probed whether Aβ fibril-doped biological samples can be accurately quantified using this assay. Known amounts of $A\beta_{1-40}$ amyloid fibrils were added to wild-type (WT) mouse brain homogenate samples (nontransgenic), and then the mixture was sonicated in a water bath sonicator and added to an $A\beta_{1-40}$ monomer solution for the kinetic aggregation assay (Figure 2a). The t_{50} is shortened in proportion to the amount of fibrillar seeds added above ~40 ng/mL, but the kinetic difference becomes small when < 40 ng/mL sonicated $A\beta_{1-40}$ fibrils were added [Figure 2b (△)]. This limited sensitivity is likely a consequence of the high protein and lipid content of mouse brain. In an attempt to improve the sensitivity and linearity of the assay, proteinase K (PK) was used to digest the soluble proteome within the brain homogenate. There is ample precedent that amyloid fibrils are resistant to PK digestion (*37*−*40*). We verified that when mouse brain homogenate was incubated with PK, the amount of soluble protein remaining was decreased dramatically (Figure S3 of the Supporting Information). We then confirmed that Aβ amyloid is PK resistant under the conditions used herein by quantifying total $A\beta_{1-40}$ following PK digestion by RP HPLC; 84% of $A\beta_{1-40}$ remains undigested following incubation with PK for 2 h (Figure S4a,b of the Supporting Information).

Wild-type mouse brain homogenate spiked with $A\beta_{1-40}$ amyloid prepared in vitro was first sonicated in a water bath sonicator for 40 min and then incubated with PK for 2 h at 25 °C. Roche complete protease inhibitor cocktail (PI) was then added to block PK activity (to prevent degradation of the initially monomeric $A\beta_{1-40}$ readout peptide used in the kinetic aggregation assay). The PK-treated mouse brain homogenate was then sonicated again in a water bath sonicator for 20 min before being added to the kinetic aggregation assay (Figure 2c). PK treatment substantially improves the sensitivity at < 40 ng/mL of added sonicated $A\beta_{1-40}$ fibrils and the linearity of the decrease in t_{50} values with an increasing amount of added seeds [Figure 2b (◆)]. It is notable that the t_{50} difference as a function of added amyloid seed is greater in the PK-treated samples (cf. Figure 2c to Figure 2a), also reflected by the increase in slope in Figure 2b. A p value of < 0.005 is realized upon comparison of the mean t_{50} values in the absence and presence of Aβ seeds (0.043 ng/mL, denoted with an asterisk in Figure 2b) utilizing the PK treatment protocol (◆). In contrast, a p value of > 0.8 is observed when the mean t_{50} values obtained in the absence and presence (0.043 ng/mL) of Aβ seeds are compared without PK treatment (△). This increased sensitivity and improved linearity of the kinetic aggregation assay utilizing the PK treatment protocol allowed quantification of added amyloid in the range of 0.04−40 ng/mL. This assay is at least 3 orders of magnitude more sensitive than the SDS−PAGE/Western blot analysis using the 6E10 antibody [cf. the ability to detect fibrils in Figure 2d to that in Figure 2b (◆)]. No antigen retrieval protocol was employed, which should increase the sensitivity of the Western blot approach.

Similarly, PK treatment of WT *C. elegans* post-debris supernatant (PDS), spiked with known amounts of $A\beta_{1-40}$ fibril seed [in Figure 3a, cf. PK-treated (◆) to untreated (△)], markedly enhances the assay sensitivity and linearity of the kinetic aggregation assay. A p value of < 0.004 is realized upon comparison of the mean t_{50} values in the absence and presence (0.43 ng/mL) of Aβ seeds (denoted with an asterisk in Figure 3a) utilizing the PK treatment protocol (◆). In contrast, a p value > 0.07 between the mean t_{50} values in the absence and the presence (0.43 ng/mL) of Aβ seeds is observed without PK treatment (△). The *C. elegans* kinetic aggregation assay is at least 3 orders of magnitude more sensitive than employing a SDS−PAGE/6E10 antibody-based Western blot approach for Aβ fibril detection [cf. Figure 3b to Figure 3a (◆)]. No antigen retrieval protocol was employed, which should increase the sensitivity of the Western blot approach.

Detection of Aβ Amyloid in an Alzheimer's Transgenic Mouse Brain Homogenate. We next examined whether the kinetic aggregation assay can be employed to semiquantify Aβ fibrils formed in vivo that differ from fibrils formed in vitro because of the bound amyloid P component and bound extracellular matrix components (such as glycosaminoglycans). We compared brain homogenates from WT mice to those from a well-characterized human transgenic Alzheimer's Aβ mouse model that shows slow progressive age-onset Aβ fibril formation in the brain (*6*, *41*).

Without PK treatment, the aggregation t_{50} values of the WT and Borchelt Alzheimer's mouse brain homogenates are not distinguishable (Figure 4a), suggesting that the proteins and lipids mask the seeding capabilities of the Aβ fibrils present in the AD mouse brains. After PK treatment to digest the soluble mouse brain proteome, differences in the kinetic aggregation assay t_{50} values between the AD and WT murine samples are

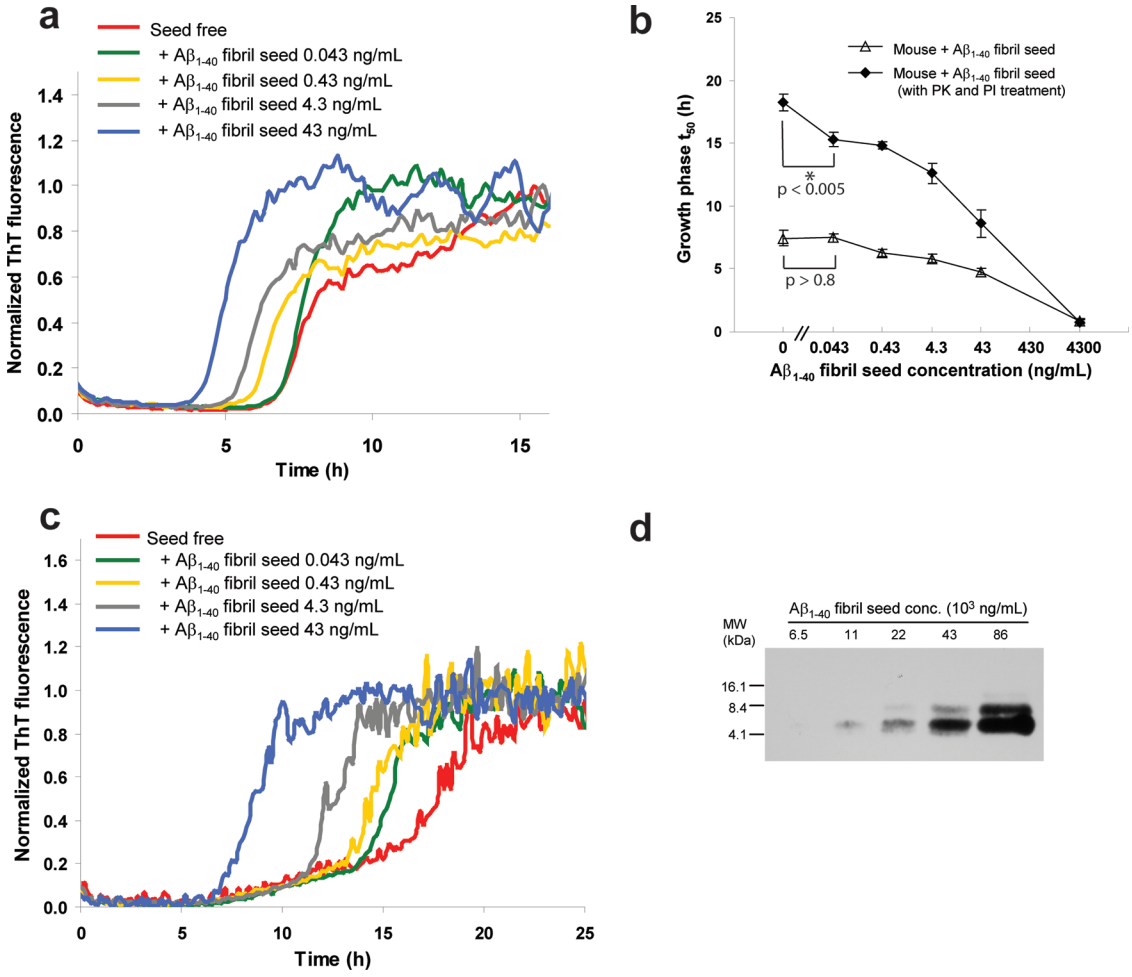

FIGURE 2: $A\beta_{1-40}$ kinetic aggregation assay to which WT mouse brain homogenate (spiked with a known amount of preformed and sonicated $A\beta_{1-40}$ amyloid fibrils) had been added. (a) $A\beta_{1-40}$ (10 μM) kinetic aggregation traces detected by ThT fluorescence (pH 7.4, 37 °C) with agitation (shaking for 5 s every 10 min) in the absence and presence of known quantities of preformed $A\beta_{1-40}$ fibril seeds (0.043−43 ng/mL) added to mouse brain tissue. Fluorescence is normalized to the value of the plateau phase in a given reaction. The mouse brain homogenate without or with added $A\beta$ fibrils was sonicated for 40 min before being added to the kinetic aggregation assay. (b) Comparison of $A\beta_{1-40}$ amyloidogenesis t_{50} values without (△) or with (◆) PK and PI pretreatment. Data are reported as means ± SD of triplicate experiments. A p value of < 0.005 is realized upon comparison of the mean t_{50} values in the absence and presence (0.043 ng/mL) of $A\beta$ seeds (denoted with an asterisk) utilizing the PK and PI treatment protocol (◆). In contrast, a p value of > 0.8 is observed when the t_{50} mean values obtained in the absence and presence (0.043 ng/mL) of $A\beta$ seeds are compared without PK and PI treatment (△). (c) $A\beta_{1-40}$ kinetic aggregation traces of PK-treated mouse brain tissue in the absence and presence of known quantities of preformed $A\beta_{1-40}$ fibril seeds. The mouse homogenate without or with added $A\beta$ fibrils was sonicated for 40 min, treated with PK for 2 h (w/w ratio of PK to total protein in the mouse brain sample of 1:500), inhibited by Roche protease inhibitor cocktail (PI) at a concentration 4 times the recommended concentration, and then sonicated for an additional 20 min before being added to the kinetic aggregation assay. (d) Dilution series of $A\beta_{1-40}$ amyloid spiked into WT mouse brain tissue as detected by Western blot analysis using the 6E10 antibody (antigen retrieval procedures not employed).

evident (Figure 4b). Addition of AD mouse brain homogenate results in a faster aggregation time course relative to that of the WT mouse brain homogenate (Figure 4b), consistent with seeding by $A\beta$ amyloid known to be present in the murine AD transgenic tissue.

Thermal Denaturation of PK To Optimize Detection of Aβ Amyloid in AD Mouse Brain. We hypothesized that heating might more fully inactivate PK and likely other proteases present in the murine brain homogenate relative to protease inhibitor cocktail treatment, improving the kinetic aggregation assay. To determine the effect of the thermal pretreatment alone on $A\beta$ fibril seeding capacity, we sonicated preformed seeds for 40 min, diluted them to concentrations ranging from 0.043 to 4300 ng/mL, heated the seeds in a boiling water bath for 10 min, and sonicated them for an additional 20 min before adding the resulting seeds to the $A\beta_{1-40}$ kinetic aggregation assay. Heating various quantities of preformed $A\beta$ fibrils in buffer leads to a decrease in their seeding capacity (Figure S5 of the Supporting Information), but this effect is nominal compared to the sensitivity gained by PK pretreatment and subsequent thermal inactivation (Figure 4c). We next sonicated mouse brain homogenates for 40 min, treated them with PK, and thermally denatured the PK by heating as described above. Samples were sonicated for an additional 20 min and added to the kinetic aggregation assay. There is a greater kinetic distinction between the boiled AD and WT murine brain homogenates relative to the PI-treated samples (cf. Figure 4c, red vs gray, to Figure 4b, red vs blue). We surmise that heating improves the kinetic aggregation assay because it more completely prevents PK, and perhaps other endogenous enzymes, from degrading the monomeric $A\beta_{1-40}$ readout peptide. This improved protocol, relative to that published previously (*6*), demonstrates that the AD mice with half the amount of insulin growth factor receptor signaling (*AD;Igf1r+/−*) exhibit a statistically significant decrease in their t_{50} values relative to those of AD mice ($p < 0.013$) (in Figure 4c, cf. yellow vs gray traces).

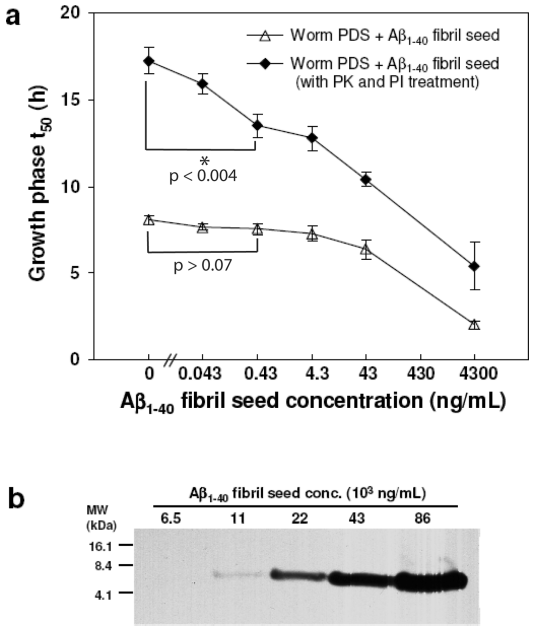

FIGURE 3: $A\beta_{1-40}$ kinetic aggregation assay utilizing WT *C. elegans* worm PDS with known quantities of preformed $A\beta_{1-40}$ fibrils added as seeds. (a) Amyloidogenesis t_{50} values of an $A\beta_{1-40}$ kinetic aggregation assay without or with the addition of known quantities of $A\beta$ fibrils added to worm PDS. The assay was performed as described in the legend of Figure 2. Triplicate data are reported as means ± SD. A p value of < 0.004 is observed upon comparison of the mean t_{50} values in the absence and presence (0.43 ng/mL) of $A\beta$ seeds (denoted with an asterisk) utilizing the PK and PI treatment protocol (◆). In contrast, a p value of > 0.07 between the mean t_{50} values in the absence and presence (0.43 ng/mL) of $A\beta$ seeds is observed without PK and PI treatment (△). (b) Dilution series of $A\beta_{1-40}$ amyloid spiked into worm PDS as detected by Western blot analysis using the 6E10 antibody (antigen retrieval procedures not employed).

These results demonstrate that *AD;Igf1r+/−* mouse brain, exhibiting protection from proteotoxicity, harbors more seeding-competent $A\beta$ amyloid than the AD mouse brain, strictly analogous to the results of our Igf1r RNAi experiments in *C. elegans* (*5*, *6*).

To estimate the quantity of amyloid in the Alzheimer's transgenic mouse samples, we chose to express the results in terms of "synthetic fibril equivalents of amyloid", rather than absolute amounts, because $A\beta$ amyloid in the Alzheimer's transgenic sample would have glycosaminoglycans, amyloid P component, and potentially other accessory molecules bound to it. These accessory molecules are less likely to accompany the amyloid in the nontransgenic mouse brain sample doped with $A\beta$ fibrils, wherein the standard curve for quantification was generated. To control for day-to-day assay variation (t_{50} variation), we normalized the t_{50} values of WT mouse homogenates spiked with known quantities of synthetic $A\beta$ seeds to the t_{50} of the control sample, the WT mouse brain homogenate sample without $A\beta$ seeds added. The normalized t_{50} values of the transgenic mouse samples (corrected relative to the t_{50} values of WT mouse samples obtained in the same assay) were compared to the normalized t_{50} values of WT mouse homogenates spiked with known quantities of synthetic $A\beta$ seeds (the source of the standard curve for quantification), yielding the synthetic fibril equivalents of amyloid in the transgenic sample. The normalized t_{50} from the AD transgenic mouse sample corresponds to 0.5 ng/mL synthetic fibril equivalents of amyloid. The estimated level of synthetic fibril equivalents of amyloid in the original mouse brain

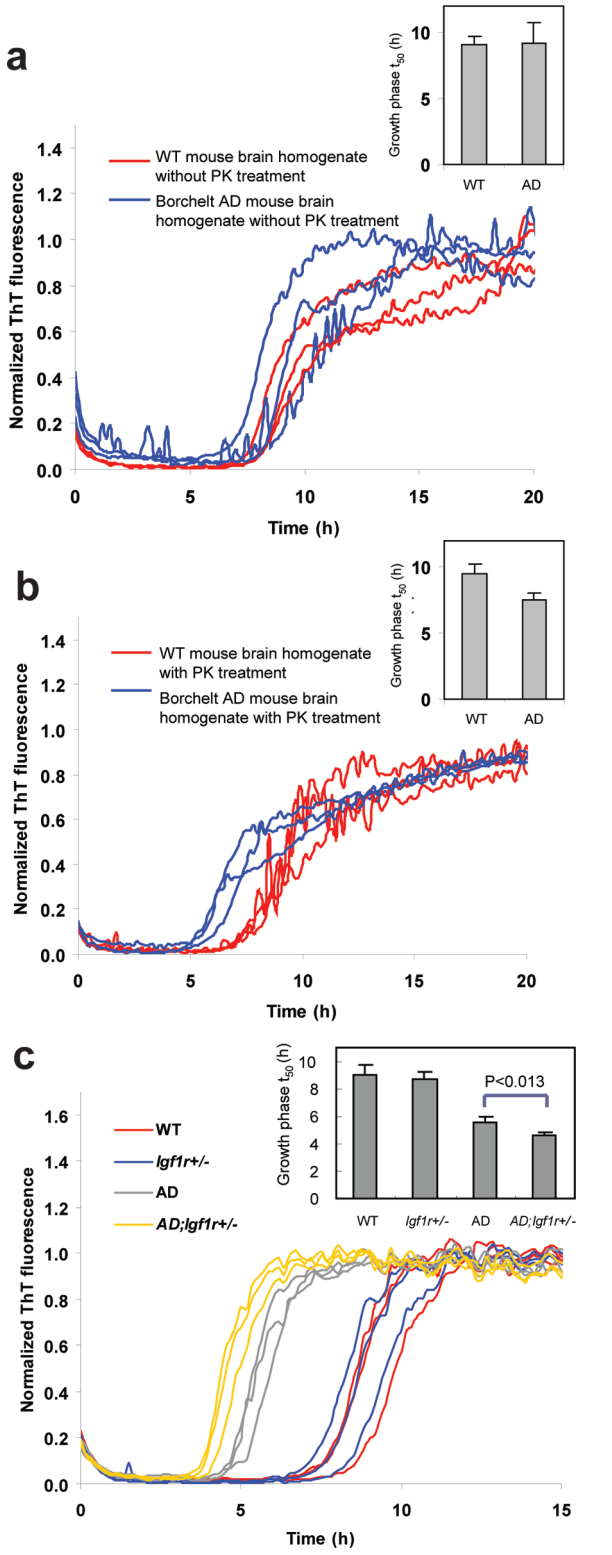

FIGURE 4: $A\beta_{1-40}$ kinetic aggregation traces with added mouse brain homogenate. Triplicate results are shown in each panel. (a) Wild type (WT) or AD mouse brain homogenate without PK treatment. The inset shows t_{50} values of the kinetic aggregation traces. Data are reported as means ± SD of triplicate results. (b) WT or AD mouse brain homogenate with PK and PI treatment. The inset shows t_{50} values of the kinetic aggregation traces with data reported as means ± SD of triplicate results. (c) WT, *Igf1r+/−*, AD, and *AD;Igf1r+/−* mouse brain homogenates with PK and thermal denaturation treatment. The mouse brain homogenates were sonicated for 40 min, treated with PK for 2 h, boiled for 10 min, sonicated for an additional 20 min, and added to the $A\beta_{1-40}$ kinetic aggregation assay. The inset shows t_{50} values of the kinetic aggregation traces with data reported as means ± SD [$p < 0.013$ between AD and *AD;Igf1r+/−* (analyzed using a two-tailed Student's t test)].

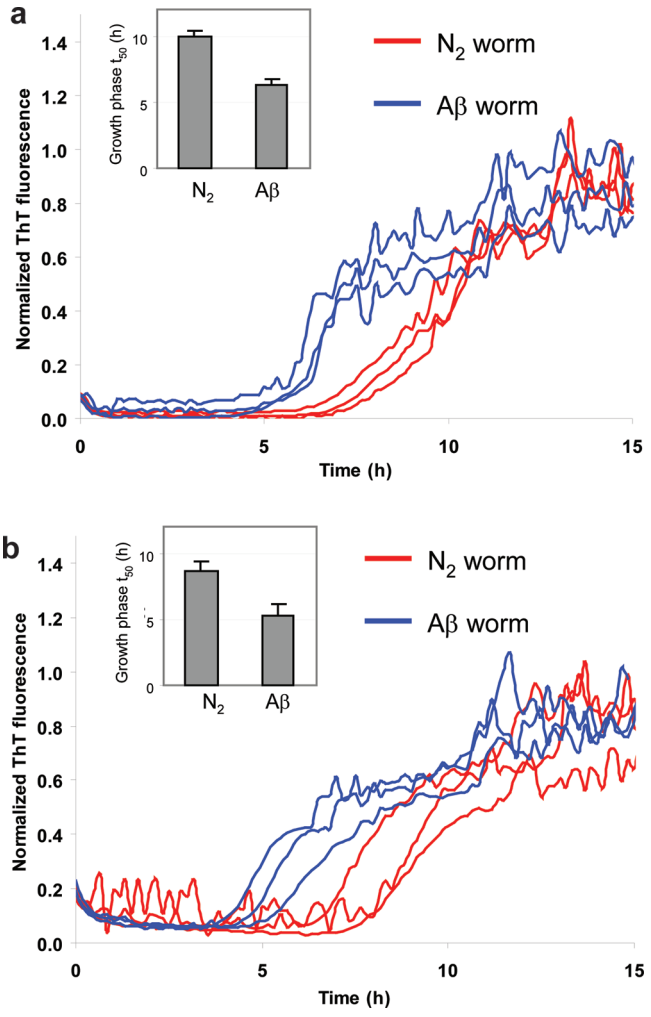

FIGURE 5: $A\beta_{1-40}$ kinetic aggregation assay with added wild-type (N_2) or Aβ worm PDS with PK and PI pretreatment (a) or without PK and PI pretreatment (b). Triplicate results are shown in each figure. The assay was performed as described in the legend of Figure 2 except that the worm samples were sonicated for only 20 min before PK treatment. Insets show statistical analysis of results obtained in panel a ($p < 0.005$) and panel b ($p < 0.013$), with data reported as means ± SD.

homogenate is ~250 ng/mL, as the mouse brain homogenate is diluted 500-fold in the kinetic aggregation assay.

Optimization of Aβ Amyloid Detection in the Alzheimer's Aβ Worm Model. Wild-type worms (N_2) not expressing Aβ and transgenic Aβ worms expressing $A\beta_{1-42}$ in the secretory system (*5*) and apparently in the cytosol were compared to discern whether PK treatment improved the ability of the kinetic aggregation assay to differentiate these samples, in comparison to our previously reported assay (*5*). PDS from N_2 and Aβ worms was sonicated for 20 min, treated with PK for 2 h at 25 °C, and then treated with Roche protease inhibitor cocktail. The mixed solution was sonicated for an additional 20 min and then added to the $A\beta_{1-40}$ readout peptide. While PK treatment (Figure 5a) does not noticeably increase the differences in t_{50} relative to those without PK treatment (Figure 5b), this step clearly reduces the uncertainty between replicated results, thus improving the sensitivity of the kinetic aggregation assay in detecting Aβ aggregates in PDS samples. We also evaluated whether thermal denaturation instead of PI treatment further improves the sensitivity. While thermal treatment reduces the differences in t_{50} between WT and AD worms, the reproducibility of the replicates improves

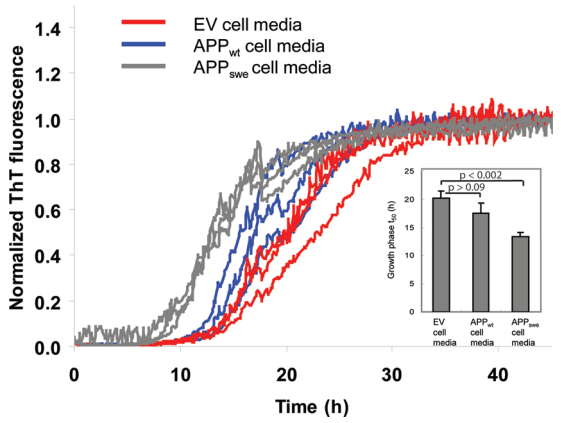

FIGURE 6: $A\beta_{1-40}$ kinetic aggregation traces with added conditioned cell media after PK and PI pretreatment (results shown in triplicate). Cells were treated with tetracycline for 4 days to induce APP expression. Tetracycline-treated EV cells do not overexpress APP, whereas APP_{wt} cells overexpress APP_{wt}; APP_{swe} cells overexpress APP_{swe} and Aβ. The assay was performed as described for the worm samples. The inset shows statistical analysis of results reported as means ± SD between EV and APP_{wt} cells ($p > 0.09$) and between EV and APP_{swe} cells ($p < 0.002$).

(cf. Figure S6a to Figure S6b of the Supporting Information), suggesting further optimization using a thermal denaturation step could prove useful.

We also estimated the quantity of amyloid in the Alzheimer's transgenic worm samples, again using the synthetic fibril equivalents of amyloid approach. As discussed in detail above, we normalized the t_{50} values obtained in kinetic aggregation assays run on different days to the t_{50} of WT worm PDS without Aβ added as the control. The normalized t_{50} of the Aβ worm PDS sample corresponds to 9.6 ng/mL synthetic fibril equivalents of amyloid. The estimated level of synthetic fibril equivalents of amyloid in the original Aβ worm PDS sample is ~3.8 μg/mL, as the Aβ worm PDS sample is diluted 400-fold in the kinetic aggregation assay.

Detection of Aβ Amyloid in Mammalian Cell Culture Media. We also explored the ability of the $A\beta_{1-40}$ kinetic aggregation assay to detect Aβ amyloid outside of the cell, using stably transfected T-REx-293 cell lines expressing empty vector (EV), WT APP (APP_{wt}), or APP_{swe}. Western blot analysis of the conditioned media revealed the presence of APP and Aβ peptide in the culture media of the tetracycline-induced T-REx-293 APP_{swe} cell line, while only APP (no Aβ) was detected in the T-REx-293 APP_{wt}-conditioned media (Figure S7a of the Supporting Information). Endogenous background levels of APP, but not Aβ, were detected in the EV cell culture media. A significant difference was observed after PK and PI treatment between the seeding efficiency of EV cell media and APP_{swe} cell media after overexpression for 4 days ($p < 0.002$) (Figure 6). However, the difference between EV cell media and APP_{wt} cell media is less distinct ($p > 0.09$), as expected. These data demonstrate that the Aβ peptides in the APP_{swe} cell culture media exist in an aggregated seeding-competent state. Without PK treatment, the distinction in the kinetic aggregation assay between APP_{swe} and EV cells is much smaller (Figure S7b of the Supporting Information).

Aβ Amyloid Isolation Using an Ion-Exchange Resin To Improve the Kinetic Aggregation Assay. We also explored a complementary method that uses an ion-exchange resin to bind amyloid from sonicated tissue extracts and cell lysates, allowing

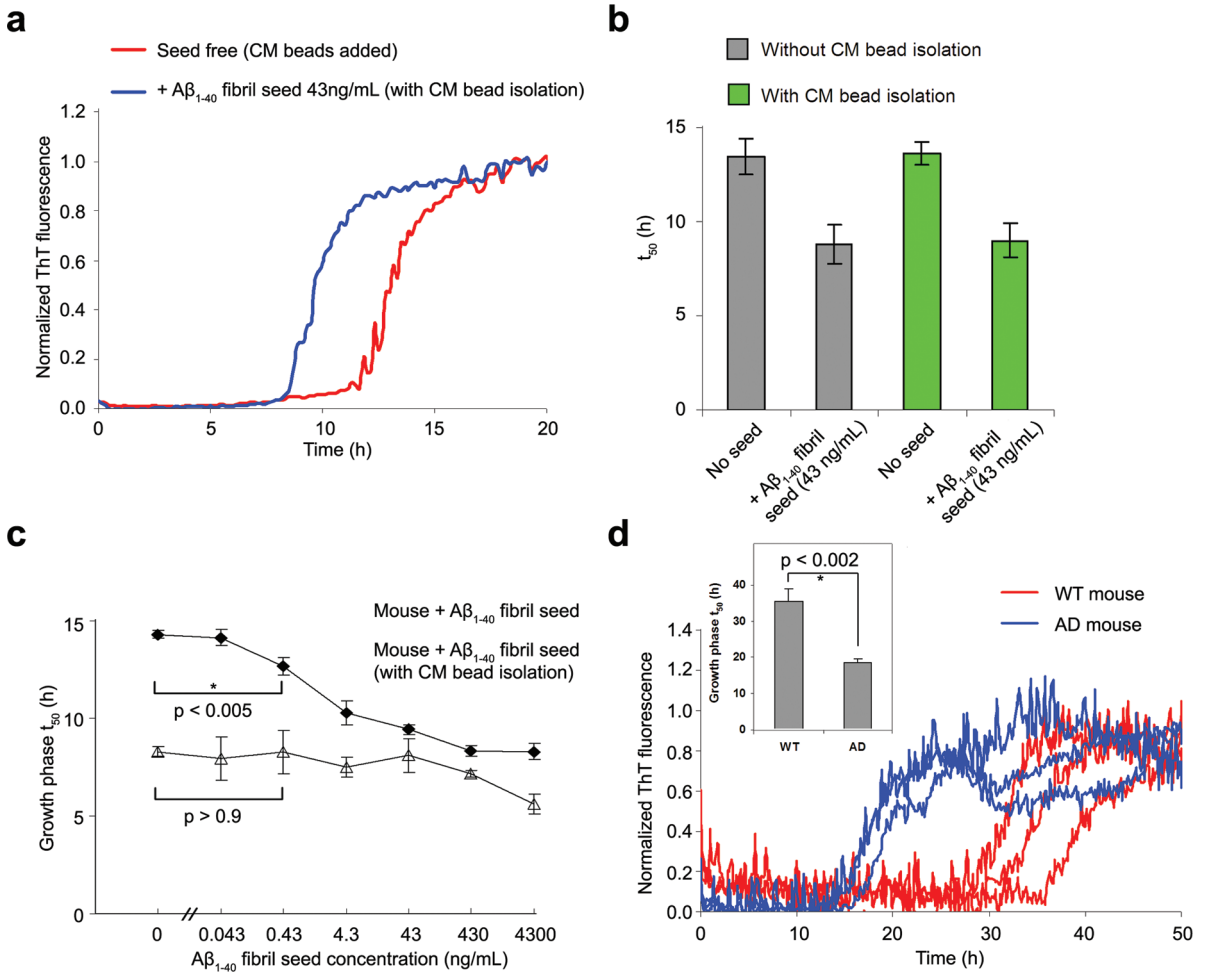

FIGURE 7: Ion-exchange resin amyloid isolation approach to the Aβ_{1-40} kinetic aggregation assay. (a) CM cation-exchange beads were incubated at 4 °C with shaking overnight without (red curve) or with (blue curve) Aβ_{1-40} fibril seeds (13 ng) and then washed with H_2O before being added to the Aβ_{1-40} kinetic aggregation assay. (b) Comparison (t_{50}) of the Aβ_{1-40} sonicated fibrils added directly to the Aβ_{1-40} readout peptide (short gray bar) vs sonicated fibrils preincubated with CM beads and washed before being added to the Aβ_{1-40} readout peptide (short green bar). Data are reported as means ± SD of triplicate experiments. (c) Comparison of the Aβ_{1-40} (10 μM) amyloidogenesis t_{50} values using the CM resin amyloid isolation strategy vs mouse brain homogenate doped with known fibril concentrations (sonication but no PK treatment). Data are reported as means ± SD of triplicate results. CM beads (8 μL) were incubated with mouse brain homogenates doped with known quantities of Aβ_{1-40} fibril seeds at 4 °C with shaking overnight, washed, and added to the Aβ_{1-40} kinetic aggregation assay. A p value of < 0.005 is realized upon comparison of the mean t_{50} values in the absence and presence (0.43 ng/mL) of Aβ seeds (denoted with an asterisk) utilizing the CM ion-exchange bead protocol (◆). In contrast, a p value of > 0.9 is observed when the t_{50} values obtained in the absence and presence (0.43 ng/mL) of Aβ seeds are compared without utilizing the CM bead approach (△, no PK treatment). (d) Differentiating WT mouse brain (red curves) from AD mouse brain (blue curves) using the CM bead amyloid isolation approach (triplicate results reported). Before CM beads were added to the readout peptide in the kinetic aggregation assay, the beads were loaded with amyloid (if present) by incubation at 4 °C with WT or AD mouse brain homogenate (total protein concentration of 50 μg/mL) with shaking overnight, followed by a washing protocol. The inset shows t_{50} values of the growth phases reported as means ± SD. A p value of < 0.002 is noted between WT and AD (denoted with an asterisk).

contaminating lipids, proteins, etc., that attenuate t_{50} differences in the kinetic aggregation assay to be washed away. Apart from making the assay easier to perform, this approach also has the capacity to concentrate the Aβ aggregates to enhance the sensitivity of the kinetic aggregation assay. First, we tested the ability of the ion-exchange resin to bind amyloid fibrils by preincubating weak cation-exchange beads (CM Sepharose fast flow, GE) with preformed sonicated Aβ fibrils before adding the beads to the kinetic aggregation assay. Unlike the CM beads that are incubated with buffer only, CM beads preincubated with Aβ fibrils significantly decrease the t_{50} of the growth phase of the kinetic aggregation assay (Figure 7a), demonstrating that the CM beads bind amyloid that can seed the kinetic aggregation assay. The seeding activity of the Aβ fibrils isolated using the CM beads is equivalent to simply adding the same quantity of sonicated fibrils directly to the kinetic aggregation assay (Figure 7b). The t_{50} of the seeded Aβ (10 μM) kinetic aggregation assay in buffer, where the seeds are presented directly, is identical to the t_{50} of the seeded kinetic aggregation assay where the seeds are absorbed to and presented on beads (cf. shorter green and gray bars in Figure 7b). Moreover, adding beads only or nothing to an Aβ (10 μM) kinetic aggregation assay in buffer affords identical kinetics (cf. taller gray and green bars in Figure 7b), demonstrating that the beads have no effect on the unseeded t_{50}.

Furthermore, if the quantity of the bead slurry employed is increased relative to a fixed amount of Aβ seeds, the t_{50} remains unchanged (Figure S8 of the Supporting Information), demonstrating that the beads have no influence on the t_{50}. Specifically, 5, 8, and 10 μL of CM bead slurry was employed with a fixed amount of Aβ fibrils (43 ng/mL), and statistically significant changes in t_{50} values in the kinetic aggregation assay in buffer were not observed, indicating that the beads were not overloaded

with Aβ seeds. Thus, CM beads can bind Aβ fibrils efficiently, very likely because of the electrostatic interactions between the CM beads and the positive charges lined up on the surface of the parallel in-register cross-β-sheet amyloid fibrils.

Next, we tested the ability of CM beads to bind to Aβ fibrils added to WT mouse brain homogenate. Analogous to the enhanced sensitivity obtained with PK treatment, CM bead amyloid isolation increases the sensitivity of the kinetic aggregation assay relative to that without CM bead amyloid isolation (Figure 7c). A p value of < 0.005 is realized upon comparison of the mean t_{50} values in the absence and presence (0.43 ng/mL) of Aβ seeds (denoted with an asterisk in Figure 7c) utilizing the CM bead amyloid isolation protocol (◆). In contrast, a p value of > 0.9 is observed without using the CM bead protocol (△), all else being equivalent.

Amyloid isolated from AD mouse brain homogenates using CM beads leads to significantly faster aggregation kinetics compared to the kinetics after treatment of WT mouse brain homogenates with CM beads (Figure 7d). Taken together, these results suggest that the kinetic aggregation assay can be further optimized using ion-exchange resins to isolate amyloid from complex biological samples.

The unseeded (0 ng/mL) Aβ (10 μM) aggregation t_{50} values in Figure 7c differ between untreated mouse brain postnuclear supernatant (PNS) and the CM resin-treated mouse brain PNS because only in the latter case are the additional brain components removed by resin washing steps, slowing the kinetics. In other words, there are effectively no brain components in the aggregation time course data depicted by the filled diamonds in Figure 7c. In contrast, in the data depicted as empty triangles, brain PNS is added directly to the Aβ (10 μM) kinetic aggregation assay; hence, it is faster, possibly because of the brain lipids.

DISCUSSION

Quantification of the amyloid load in tissues remains challenging and is important for improving our understanding of the etiology of degenerative diseases (*1*−*3*, *42*−*51*). Selective and sensitive detection of small quantities of specific amyloid fibrils formed in the early stages of disease is of special interest, as this offers diagnostic opportunities (*37*, *38*, *52*). Previously, we used an Aβ_{1-40} kinetic aggregation assay to detect amyloid in worm PDS (*5*); however, this method was semiquantitative. We have demonstrated herein that we can selectively, sensitively, and quantitatively detect Aβ amyloid load in a variety of cell and tissue homogenates using the optimized Aβ kinetic aggregation assay. A future goal is to render the kinetic aggregation assay rigorously quantitative in mouse and worm PDS, where accessory factors can complicate quantification relative to analogous samples in which known quantities of amyloid are added. It will be very interesting in the future to discern how well the synthetic fibril equivalents of amyloid correlate with the absolute amount of amyloid in a transgenic AD model.

A challenge in quantifying low levels of amyloid in biological samples is that amyloid fibrils are minor components of an environment densely packed with small molecule metabolites; macromolecules, including proteins, RNA, and DNA; and lipids and other membrane components. Moreover, the amyloid P component (*53*) and glycosaminoglycans (*54*) are known to selectively bind to the surface of amyloid fibrils, potentially masking their presence. These interactions could stabilize the amyloid fibrils and interfere with sonication to break up the fibrils into smaller seeds and/or sterically interfere with the seeding activity of sonicated amyloid seeds. In spite of not removing glycosaminoglycans or membrane components, removal of soluble proteins using PK treatment dramatically improves the sensitivity and the linear response of the kinetic aggregation assay, as does an ion-exchange resin amyloid isolation strategy, which may be more practical to utilize as the beads with absorbed amyloid seeds can be added directly to the readout peptide. We envision that enzymatic degradation of sulfated glycosaminoglycans and membrane/lipid extraction will have the potential to further improve the Aβ_{1-40} kinetic aggregation assay, allowing us to move closer to our goal of rigorously quantifying the Aβ amyloid load in tissues and biological fluids.

One potential advantage of the ion-exchange resin approach is that the amyloid in complex biological samples like cerebrospinal fluid (CSF) can be concentrated on the ion-exchange resin surface, enhancing the capacity to detect amyloid using the kinetic aggregation assay. However, attempts to detect kinetic differences between Alzheimer's and age-matched control human CSF and blood plasma samples [obtained from D. Holtzman (Washington University, St. Louis, MO)] using the kinetic aggregation assay have been unsuccessful to date. The substantial effort put into this suggests that the concentration of Aβ fibrils in Alzheimer's human CSF and blood plasma samples is very low, if present at all, and certainly below the detection limits of the current kinetic aggregation assay. Further optimization of the methodology to enhance the sensitivity may allow the assay to detect very small quantities of Aβ fibrils present in easily accessible human samples.

It should be noted that distinct biological samples required different optimized kinetic aggregation assays, presumably because of their unique molecular composition. For example, while PK treatment to remove interfering soluble proteins was generally useful, thermal treatment to inactivate PK and possibly other proteases significantly improved the mouse brain kinetic aggregation assay but did not enhance the ability to detect Aβ amyloid in cell culture media and only modestly improved detection of Aβ amyloid in *C. elegans*. From the perspective of practicality and ease of use, the ion-exchange resin amyloid isolation approach is perhaps the most promising strategy for further enhancing the kinetic aggregation assay; however, future experiments are required to see if its promise can be realized experimentally.

CONCLUSION

We have outlined the basis for improved Aβ_{1-40} kinetic aggregation assays and demonstrated their general utility for the quantitative or semiquantitative, sensitive, and selective detection of Aβ amyloid load in a variety of organismal fractions, including mouse brain homogenate, worm PDS, and cell culture media. Proteinase K treatment substantially improves the sensitivity and linearity of the Aβ_{1-40} kinetic aggregation assay in most organismal fractions. Thermal inactivation of proteinase K, and likely other proteases, further enhances the utility of the Aβ_{1-40} kinetic aggregation assay, especially in mammalian tissue. Further optimization of the Aβ_{1-40} kinetic aggregation assay, perhaps using the ion-exchange resin amyloid isolation strategy presented herein, should render it even more practical and quantitative, possibly allowing it to detect the presence of Aβ fibrils in human CSF or other accessible fluids or tissues for diagnostic purposes. We envision that any amyloid protein that

aggregates in vitro by a nucleated polymerization reaction can be used as a readout peptide in a kinetic aggregation assay to quantify the amyloid load of that peptide in a given tissue or body fluid.

SUPPORTING INFORMATION AVAILABLE

Experimental procedures for genotyping of mice, APP-overexpressing lines, and AFM and supplementary figures as mentioned in the text. This material is available free of charge via the Internet at http://pubs.acs.org.

REFERENCES

1. Tanzi, R. E., and Bertram, L. (2005) Twenty years of the Alzheimer's disease amyloid hypothesis: A genetic perspective. *Cell 120*, 545–555.
2. Hardy, J., and Selkoe, D. J. (2002) Medicine: The amyloid hypothesis of Alzheimer's disease: Progress and problems on the road to therapeutics. *Science 297*, 353–356.
3. Golde, T. E., Estus, S., Younkin, L. H., Selkoe, D. J., and Younkin, S. G. (1992) Processing of the amyloid protein precursor to potentially amyloidogenic derivatives. *Science 255*, 728–730.
4. Amaducci, L., and Tesco, G. (1994) Aging as a major risk for degenerative diseases of the central nervous system. *Curr. Opin. Neurol. 7*, 283–286.
5. Cohen, E., Bieschke, J., Perciavalle, R. M., Kelly, J. W., and Dillin, A. (2006) Opposing activities protect against age-onset proteotoxicity. *Science 313*, 1604–1610.
6. Cohen, E., Paulsson, J. F., Blinder, P., Burstyn-Cohen, T., Du, D., Estepa, G., Adame, A., Pham, H. M., Holzenberger, M., Kelly, J. W., Masliah, E., and Dillin, A. (2009) Reduced IGF-1 signaling delays age-associated proteotoxicity in mice. *Cell 139*, 1157–1169.
7. Braak, E., Braak, H., and Mandelkow, E. M. (1994) A sequence of cytoskeleton changes related to the formation of neurofibrillary tangles and neuropil threads. *Acta Neuropathol. 87*, 554–567.
8. Lee, V. M., Balin, B. J., Otvos, L. J., and Trojanowski, J. Q. (1991) A68: A major subunit of paired helical filaments and derivatized forms of normal Tau. *Science 251*, 675–678.
9. Balch, W. E., Morimoto, R. I., Dillin, A., and Kelly, J. W. (2008) Adapting proteostasis for disease intervention. *Science 319*, 916–919.
10. Powers, E. T., Morimoto, R. I., Dillin, A., Kelly, J. W., and Balch, W. E. (2009) Biological and chemical approaches to diseases of proteostasis deficiency. *Annu. Rev. Biochem. 78*, 959–991.
11. Gidalevitz, T., Krupinski, T., Garcia, S., and Morimoto, R. I. (2009) Destabilizing protein polymorphisms in the genetic background direct phenotypic expression of mutant SOD1 toxicity. *PLoS Genet. 5*, e1000399.
12. Gidalevitz, T., Ben-Zvi, A., Ho, K. H., Brignull, H. R., and Morimoto, R. I. (2006) Progressive disruption of cellular protein folding in models of polyglutamine diseases. *Science 311*, 1471–1474.
13. Page, L. J., Suk, J. Y., Bazhenova, L., Fleming, S. M., Wood, M., Jiang, Y., Guo, L. T., Mizisin, A. P., Kisilevsky, R., Shelton, G. D., Balch, W. E., and Kelly, J. W. (2009) Secretion of amyloidogenic gelsolin progressively compromises protein homeostasis leading to the intracellular aggregation of proteins. *Proc. Natl. Acad. Sci. U.S.A. 106*, 11125–11130.
14. Klunk, W. E., Engler, H., Nordberg, A., Wang, Y., Blomqvist, G., Holt, D. P., Bergstrom, M., Savitcheva, I., Huang, G. F., Estrada, S., Ausen, B., Debnath, M. L., Barletta, J., Price, J. C., Sandell, J., Lopresti, B. J., Wall, A., Koivisto, P., Antoni, G., Mathis, C. A., and Langstrom, B. (2004) Imaging brain amyloid in Alzheimer's disease with Pittsburgh Compound-B. *Ann. Neurol. 55*, 306–319.
15. Kayed, R., and Glabe, C. G. (2006) Conformation-dependent anti-amyloid oligomer antibodies. *Methods Enzymol. 413*, 326–344.
16. O'Nuallain, B., and Wetzel, R. (2002) Conformational Abs recognizing a generic amyloid fibril epitope. *Proc. Natl. Acad. Sci. U.S.A. 99*, 1485–1490.
17. Edison, P., Archer, H. A., Gerhard, A., Hinz, R., Pavese, N., Turkheimer, F. E., Hammers, A., Tai, Y. F., Fox, N., Kennedy, A., Rossor, M., and Brooks, D. J. (2008) Microglia, amyloid, and cognition in Alzheimer's disease: An [11C](R)PK11195-PET and [11C]PIB-PET study. *Neurobiol. Dis. 32*, 412–419.
18. Lockhart, A., Lamb, J. R., Osredkar, T., Sue, L. I., Joyce, J. N., Ye, L., Libri, V., Leppert, D., and Beach, T. G. (2007) PIB is a non-specific imaging marker of amyloid-β (Aβ) peptide-related cerebral amyloidosis. *Brain 130*, 2607–2615.
19. Naiki, H., Hasegawa, K., Yamaguchi, I., Nakamura, H., Gejyo, F., and Nakakuki, K. (1998) Apolipoprotein E and antioxidants have different mechanisms of inhibiting Alzheimer's β-amyloid fibril formation in vitro. *Biochemistry 37*, 17882–17889.
20. Teplow, D. B. (1998) Structural and kinetic features of amyloid β-protein fibrillogenesis. *Amyloid 5*, 121–142.
21. Harper, J. D., and Lansbury, P. T. (1997) Models of amyloid seeding in Alzheimer's disease and scrapie: Mechanistic truths and physiological consequences of the time-dependent solubility of amyloid proteins. *Annu. Rev. Biochem. 66*, 385–407.
22. Ferrone, F. A. (2006) Nucleation: The connections between equilibrium and kinetic behavior. *Methods Enzymol. 412*, 285–299.
23. Powers, E. T., and Powers, D. L. (2008) Mechanisms of protein fibril formation: Nucleated polymerization with competing off-pathway aggregation. *Biophys. J. 94*, 379–391.
24. Wellings, D. A., and Atherton, E. (1997) Standard Fmoc protocols. *Methods Enzymol. 289*, 44–67.
25. Zhang, Q., Powers, E. T., Nieva, J., Huff, M. E., Dendle, M. A., Bieschke, J., Glabe, C. G., Eschenmoser, A., Wentworth, P., Jr., Lerner, R. A., and Kelly, J. W. (2004) Metabolite-initiated protein misfolding may trigger Alzheimer's disease. *Proc. Natl. Acad. Sci. U.S.A. 101*, 4752–4757.
26. Holzenberger, M., Dupont, J., Ducos, B., Leneuve, P., Geloen, A., Even, P. C., Cervera, P., and Le Bouc, Y. (2003) IGF-1 receptor regulates lifespan and resistance to oxidative stress in mice. *Nature 421*, 182–187.
27. Ban, T., Hoshino, M., Takahashi, S., Hamada, D., Hasegawa, K., Naiki, H., and Goto, Y. (2004) Direct observation of Aβ amyloid fibril growth and inhibition. *J. Mol. Biol. 344*, 757–767.
28. Andersen, C. B., Yagi, H., Manno, M., Martorana, V., Ban, T., Christiansen, G., Otzen, D. E., Goto, Y., and Rischel, C. (2009) Branching in amyloid fibril growth. *Biophys. J. 96*, 1529–1536.
29. LeVine, H., III (1999) Quantification of β-sheet amyloid fibril structures with thioflavin T. *Methods Enzymol. 309*, 274–284.
30. O'Nuallain, B., Williams, A. D., Westermark, P., and Wetzel, R. (2004) Seeding specificity in amyloid growth induced by heterologous fibrils. *J. Biol. Chem. 279*, 17490–17499.
31. Krebs, M. R., Morozova-Roche, L. A., Daniel, K., Robinson, C. V., and Dobson, C. M. (2004) Observation of sequence specificity in the seeding of protein amyloid fibrils. *Protein Sci. 13*, 1933–1938.
32. Schmidt, M., Sachse, C., Richter, W., Xu, C., Fandrich, M., and Grigorieff, N. (2009) Comparison of Alzheimer A$\beta_{(1-40)}$ and A$\beta_{(1-42)}$ amyloid fibrils reveals similar protofilament structures. *Proc. Natl. Acad. Sci. U.S.A. 106*, 19813–19818.
33. Paravastu, A. K., Leapman, R. D., Yau, W. M., and Tycko, R. (2008) Molecular structural basis for polymorphism in Alzheimer's β-amyloid fibrils. *Proc. Natl. Acad. Sci. U.S.A. 105*, 18349–18354.
34. Luhrs, T., Ritter, C., Adrian, M., Riek-Loher, D., Bohrmann, B., Dobeli, H., Schubert, D., and Riek, R. (2005) 3D structure of Alzheimer's amyloid-$\beta_{(1-42)}$ fibrils. *Proc. Natl. Acad. Sci. U.S.A. 102*, 17342–17347.
35. Jarrett, J. T., Berger, E. P., and Lansbury, P. T., Jr. (1993) The carboxy terminus of the β amyloid protein is critical for the seeding of amyloid formation: Implications for the pathogenesis of Alzheimer's disease. *Biochemistry 32*, 4693–4697.
36. Toeroek, M., Milton, S., Kayed, R., Wu, P., McIntire, T., Glabe, C. G., and Langen, R. (2002) Structural and Dynamic Features of Alzheimer's Aβ Peptide in Amyloid Fibrils Studied by Site-Directed Spin Labeling. *J. Biol. Chem. 277*, 40810–40815.
37. Atarashi, R., Moore Roger, A., Sim Valerie, L., Hughson Andrew, G., Dorward David, W., Onwubiko Henry, A., Priola Suzette, A., and Caughey, B. (2007) Ultrasensitive detection of scrapie prion protein using seeded conversion of recombinant prion protein. *Nat. Methods 4*, 645–650.
38. Saborio, G. P., Permanne, B., and Soto, C. (2001) Sensitive detection of pathological prion protein by cyclic amplification of protein misfolding. *Nature 411*, 810–813.
39. Soderberg, L., Dahlqvist, C., Kakuyama, H., Thyberg, J., Ito, A., Winblad, B., Naslund, J., and Tjernberg Lars, O. (2005) Collagenous Alzheimer amyloid plaque component assembles amyloid fibrils into protease resistant aggregates. *FEBS J. 272*, 2231–2236.
40. Tjernberg, L. O., Naaslund, J., Thyberg, J., Gandy, S. E., Terenius, L., and Nordstedt, C. (1997) Generation of Alzheimer amyloid β peptide through nonspecific proteolysis. *J. Biol. Chem. 272*, 1870–1875.
41. Jankowsky, J. L., Savonenko, A., Schilling, G., Wang, J., Xu, G., and Borchelt, D. R. (2002) Transgenic mouse models of neurodegenerative disease: Opportunities for therapeutic development. *Curr. Neurol. Neurosci. Rep. 2*, 457–464.

42. Reilly, J. F., Games, D., Rydel, R. E., Freedman, S., Schenk, D., Young, W. G., Morrison, J. H., and Bloom, F. E. (2003) Amyloid deposition in the hippocampus and entorhinal cortex: Quantitative analysis of a transgenic mouse model. *Proc. Natl. Acad. Sci. U.S.A. 100*, 4837–4842.
43. Schmidt, S. D., Nixon, R. A., and Mathews, P. M. (2005) ELISA method for measurement of amyloid-β levels. *Methods Mol. Biol. 299*, 279–297.
44. Bellotti, V., Mangione, P., and Merlini, G. (2000) Review: Immunoglobulin Light Chain Amyloidosis: The Archetype of Structural and Pathogenic Variability. *J. Struct. Biol. 130*, 280–289.
45. Comenzo, R. L. (2006) Systemic immunoglobulin light-chain amyloidosis. *Clin. Lymphoma Myeloma 7*, 182–185.
46. Golde, T. E., Dickson, D., and Hutton, M. (2006) Filling the gaps in the Aβ cascade hypothesis of Alzheimer's disease. *Curr. Alzheimer Res. 3*, 421–430.
47. Hammarstrom, P., Wiseman, R. L., Powers, E. T., and Kelly, J. W. (2003) Prevention of Transthyretin Amyloid Disease by Changing Protein Misfolding Energetics. *Science 299*, 713–716.
48. Johnson, S. M., Wiseman, R. L., Sekijima, Y., Green, N. S., Adamski-Werner, S. L., and Kelly, J. W. (2005) Native State Kinetic Stabilization as a Strategy To Ameliorate Protein Misfolding Diseases: A Focus on the Transthyretin Amyloidoses. *Acc. Chem. Res. 38*, 911–921.
49. Sekijima, Y., Wiseman, R. L., Matteson, J., Hammarstrom, P., Miller, S. R., Sawkar, A. R., Balch, W. E., and Kelly, J. W. (2005) The biological and chemical basis for tissue-selective amyloid disease. *Cell 121*, 73–85.
50. Selkoe, D. J. (2003) Folding proteins in fatal ways. *Nature 426*, 900–904.
51. Wahrle, S. E., and Holtzman, D. M. (2007) Apolipoprotein E, amyloid β peptide, and Alzheimer's disease. Neurobiology of Alzheimer's Disease, 3rd ed., pp 161−172, Oxford University Press, Oxford, U.K.
52. Colby, D. W., Zhang, Q., Wang, S., Groth, D., Legname, G., Riesner, D., and Prusiner, S. B. (2007) Prion detection by an amyloid seeding assay. *Proc. Natl. Acad. Sci. U.S.A. 104*, 20914–20919.
53. Coria, F., Castano, E., Prelli, F., Larrondo-Lillo, M., Van Duinen, S., Shelanski, M. L., and Frangione, B. (1988) Isolation and characterization of amyloid P component from Alzheimer's disease and other types of cerebral amyloidosis. *Lab. Invest. 58*, 454–458.
54. Suk, J. Y., Zhang, F., Balch, W. E., Linhardt, R. J., and Kelly, J. W. (2006) Heparin accelerates gelsolin amyloidogenesis. *Biochemistry 45*, 2234–2242.